

컴퓨터 시뮬레이션을 이용한 항만설계 및 부산항 3단계 개발
계획에 대한 응용에 관한 연구

김 환 수*

A Study on the Microcomputer Aided Port
Design Simulation and its Application to the
Third Stage Busan Port Development Project.

Whan-Soo Kim

〈CONTENTS〉

Abstract

1. INTRODUCTION

2. PORT DESIGN SIMULATION METHODOLOGY

2.1 Concept of Port Design Simulator

2.2 Mathematical Models for Simulation

2.2.1 Basic Theory of the Force Type Mathematical Model

2.2.2 Basic Theory of the Heuristic Type Mathematical Model

2.3 Accuracy and Validity of the Mathematical Model

3. APPLICATION OF SIMULATION TO THE THIRD STAGE BUSAN PORT
DEVELOPMENT PROJECT

3.1 Third Stage Development Plan for the New Container Terminal

3.2 Modelling for Simulation

3.2.1 Modelling Environmental Parameters

3.2.2 Computation of Model Equations

3.3 Preparation of Visual Scene Database and Run Schedule

3.3.1 Visual Scene and Radar Database

3.3.2 Run Schedule

3.4 Analysis of the Simulation Results

3.4.1 Unberthing Simulation in the Turning Basin

3.4.2 Entering Manoeuvres Through the new Breakwaters

3.4.3 Berthing Manoeuvres

3.4.4 Departure Manoeuvres from the Pier to the Pilot Station

4. CONCLUSIONS

REFERENCES

APPENDIX

Abstract

This work aims to introduce the concept of microcomputer aided port design simulation methodology including the analysis of the mathematical models to be implemented and apply it to the Third Stage Busan Port Development Project. In the Busan case study, the size of the proposed turning basin of the new terminal, together with the operational strategies of berthing and unberthing, was examined. In addition, the safety on ships' entry and exit through the projected new breakwaters was ascertained.

From the application of simulation to the Busan project, it was found that the proposed dredging area was not sufficiently wide enough for the modelled container ship to perform A type unberthing (in which the ship turns to port as she manoeuvres away from No. 1 berth with the assistance of tugs), especially in a strong easterly wind. It is, therefore, recommended that Busan pilots should be advised to use B type unberthing strategy, in which the ship goes astern from No. 1 berth to the turning area in front of No. 2 berth (where the ship turns 180 degrees clockwise), especially when the wind is very strong. It is also recommended that a sea buoy be placed outside the new breakwaters, as this was found to improve the safety of ship manoeuvres through the breakwaters significantly. Another recommendation is that the Korean Hydrodynamic Office carry out a detailed survey of the currents in the water area near the new breakwaters once they have been constructed. In addition, it is to be recommended that a current meter be placed at the recommended sea buoy to improve the safety of ship manoeuvres which could otherwise be jeopardised by erroneous current information.

요 약

시뮬레이션 분석 결과는 다음과 같다.

본 논문은 마이크로 컴퓨터를 이용한 항만설계 시뮬레이션에 대한 개념을 소개하고 시뮬레이션의 핵심인 선박의 수학 모델에 대해 해석 및 분석을 하였다. 그리고 항만설계 시뮬레이션 기법을 부산항 3단계 개발 계획에 직접 응용하여 본 계획과 관련한 설계상의 문제점 유무, 그리고 개발이 예정대로 완료된 후 입출항할 대형 컨테이너선의 조선과 관련된 문제점 등에 대해 검정을 하였다. 먼저, 신설되는 컨테이너 터미널 전방의 turning basin의 크기에 대해 검정하고 동시에 선박의 이접안에 대해 그 안전성을 확인하였다. 동시에 새로 건설되는 부산 외항의 방파제를 통한 선박의 입출항과 관련한 안전성 문제도 검정하였다. 시뮬레이션에는 전장 297m 총톤수 60,000톤의 panamax size의 풀 컨테이너선을 이용하였다. 시뮬레이션은 전직 카디프항 도선사와 유경험 항해사에 의해 직접 실시되었으며 총 116회의 시뮬레이션 중 68회의 시뮬레이션이 실제 문제의 분석에 이용되었다.

(1) 설계상의 12.5m 준설구역은 시뮬레이션에 도입된 컨테이너 선박이 1번 선석(제일 북쪽)으로부터 4척의 tug boat의 지원하에 왼쪽으로 회두하며 곧바로 이안하기에는 너무 좁다는 것이 밝혀졌다(특히 동풍이 강하게 부는 경우). 따라서 바람이 심하게 부는 경우에는 1번 선석으로부터 tug boat의 지원아래 곧바로 후진 이안하여 2번 선석(터미널의 가운데) 앞부분에 와서 180도 선회한 후 출항하는 방법을 취해야만 안전할 것이라는 것이 확인되었다.

(2) 모델된 컨테이너선이 신설된 방파제를 통과하여 입출항하는 데는 악조건의 환경하에서도 큰 문제점이 없다는 것이 밝혀졌다. 그러나 도선사기 승선후 방파제로 진입하는 짧은 시간동안 뚜렷한 물표가 부족함으로 인하여 초기위치 확인 및 육안에 의한 계속적이고도 정확한 위치 추정이 불가능하고 이로 인하여 바람과 조류가 강한 경우에 선박이 방파제 끝단 쪽으로 위험할 정도로 drifting

되는 경우가 있다는 점이 확인되었다.

(3) 따라서 초기 위치 확인을 돕기 위하여 동쪽 방파제의 수선과 서쪽 방파제의 연장선상에 sea buoy를 설치하여 이 buoy가 입항조선에 미치는 영향을 조사하여 보았으며 그 결과 선박의 drifting이 현저하게 감소되고 조선의 안전성이 훨씬 향상된다는 것이 확인되었다. 따라서 본 sea buoy의 설치가 강력히 권고된다.

(4) 시뮬레이션 결과 신설 방파제 부근의 조류의 속도 및 방향에 관한 정확한 정보가 입출항 선박의 안전 조선에 결정적인 역할을 한다는 것이 밝혀졌다. 따라서 방파제가 축조된 후 수로국 등에게 조류의 변화에 대해 정밀조사를 실시하여 정확한 조류정보를 도선사 등에게 제공하여야만 할 것이다. 그리고 조류 정보의 항구적인 제공방법의 하나로 위에서 제시된 sea buoy에 자동 조류 탐지기를 설치하여 선박의 안전 입출항을 도모하여야 바람직할 것이라고 본다.

(5) 새 컨테이너 터미널에 선박을 접안시키는데는 큰 어려움이 없다는 것이 확인되었으며 강한 동풍이 부는 경우에는 반드시 4척의 tug boat를 이용할 것이 권고된다.

항만설계를 위한 시뮬레이션에는 항상 최악의 환경조건을 고려하여야 하며 본 부산항 시뮬레이션에서는 바람의 경우에는 27Kts와 30Kts를 최악의 상황으로 설정하였으며 조류에 관해서는 조류도상의 정보를 이용하여 최고 조류속도 1.2Kts를 적용하였다. 그러나 조류도상의 조류속도보다 강한 조류를 체험하고 있다는 현지 도선사들의 의견에 따라 최고 2.4Kts의 조류도 시험적으로 입력하여 검정하여 보았다. 그리고 방파제가 완공된 후 조류의 크기와 방향이 변화할 것이 예상되나 본 연구에서는 경험적인 방법으로 조류의 변화를 예측하여 이를 기본 데이터로 사용하였으므로 특히 방파제 부근의 시뮬레이션 결과는 예측치의 정확도 내에서 그 신뢰성이 인정된다는 점을 밝히며, 방파제 신설후 조류 변화에 대한 정확한 조사가 매우 중요하다는 점을 다시 한번 강조한다.

NOMENCLATURE

List of Symbols

Symbol	Meaning	Units
C_L	lift coefficient	—
C_D	drag coefficient	—
d_1	surge acceleration, hull hydrodynamics	m/s
d_2	sway acceleration, hull hydrodynamics	m/s
d_3	yaw acceleration, hull hydrodynamics	rad/s
$d(1)$	total surge acceleration	m/s ²
$d(2)$	total sway acceleration	m/s ²
$d(3)$	total yaw acceleration	rad/s ²
d_f	degrees of freedom	—
D_g	helm angle	deg
D_H	drag force	N
D_R	rudder hydrodynamic drag force	N
D_{wm}	shallow water depth factor	—
I_z	moment of inertia of the ship about z_0 axis	kgm ²
K_n, K_r	new coeff. values for shallow water	—
L	length between perpendiculars	m
L_H	hull lift force	N
L_R	rudder hydrodynamic lift force	N
m	mass of the ship	kg
m_1, m_2	total mass(actual plus added mass)	kg
n	propeller rotating speed	rad/s
N	total moment of the ship about z_0 axis	kgm
N_s	shaft speed	rpm
N_{sd}	desired shaft speed	rpm
N_v	viscous damping torque about z axis	kgm
r	yaw rate	rad/s
R_c	current induced yaw rate	rad/s

ship's behaviour in conjunction with the environment and makes decisions, thereby simulating the real world situation. These decisions are transferred to the main computer through the bridge instruments ; steering wheel, engine telegraphs and bow thrusters. The main computer, which has a mathematical model of the vessel on which the simulation is taking place, is at the heart of the simulator.

Mathematical models for computer application generally take the form of a set of differential equations. These equations, when fed with inputs which represent the ship's status ; rudder angle, engine setting, and the environmental conditions such as wind, wave and currents, produce a numerical response which is similar to the response of the real vessel. A feedback loop operates between the working environment and the main computer. The main computer presents calculated output information, which is the response to the input, on the displays through which ship operators monitor the ship's behaviour. The ship operator varies the input in response to the displayed information, thereby changing the subsequent feedback.

To present the visual scene as it is seen through the windows of the ship's bridge, the image projection system is connected to the main computer. This projection system accepts signals of the observer's position in space and heading to the image projection system regarding the manoeuvring status of the vessel from the main computer. The visual scene is projected to the screen or monitor by the projection system with respect to the own vessel's position and angle of view. This presentation moves in accordance with the change of the above input from the main computer.

Input variables with regard to the own ship, other ships, instrumentation, or the simulated environment is fed in and controlled from the in-

structor's station. In addition to the instrumentation required to control a simulation, hard copy plotting facilities are used to record the results of each simulation run. Plan view plots record the visual database outline and tracks of the vessels simulated. This information becomes an integral part of the simulation analysis after the exercise is completed.

The concept of the microcomputer aided process design simulator, especially with respect to a mathematical model constructed on modular lines is described in figure 2. 1.

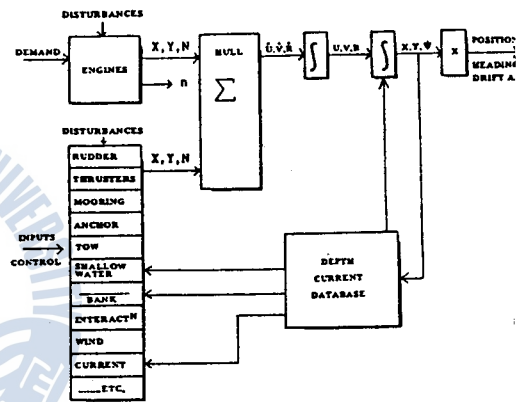


Figure 2.1 Concept of Microcomputer Aided Process Design Simulator
 - Modular Mathematical Model -
 (Source : Reference [12])

2.2 Mathematical Models for Simulation

In the simulator the real time scale response of the ship on commands from the wheelhouse is calculated by a computer and made visible through CGI screens.

Among different types of ship mathematical models developed for marine simulation, the first type model of McCallum [13], which is established under the assumption that the hydrodynamic behaviour of a ship's hull at a drift angle is directly analogous to the behaviour of a cor-

surface inclined at an angle of attack to the incoming water stream, is discussed and analysed in this section. In addition, heuristic type mathematical model is also introduced. This model contains speed, sway and engine response equations.

2.2.1 Basic Theory of the Force Type Mathematical Model

The movements of a ship on real time in the horizontal plane are described by Newtonian equations.

The forces acting on a foil set at an angle of incidence to the incoming flow can be resolved into two components, the lift L and drag D, which are normal to and along the line of incident flow respectively, as shown in figure 2.2. The angle between the face of the section and the incoming flow is the angle of incidence α . The forces are usually expressed in the form of non-dimensional coefficients as follows [15] ;

$$\begin{aligned} \text{Lift Coefficient} = C_L &= \frac{L}{\frac{1}{2}\rho AV^2} \\ \text{Drag Coefficient} = C_D &= \frac{D}{\frac{1}{2}\rho AV^2} \end{aligned} \quad (2.1)$$

where, ρ =mass density of fluid
 A =area of plan form of section
 =(chord×span) for rectangular shape
 V =velocity of incident flow

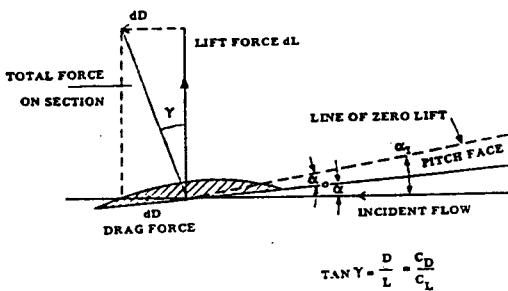


Figure 2.2 Forces on a Hydro-Foil (Source : Reference [14])

The lift and drag characteristics are shown in figure 2.3, which was reproduced from figure 84 in chapter 7 of reference [14].

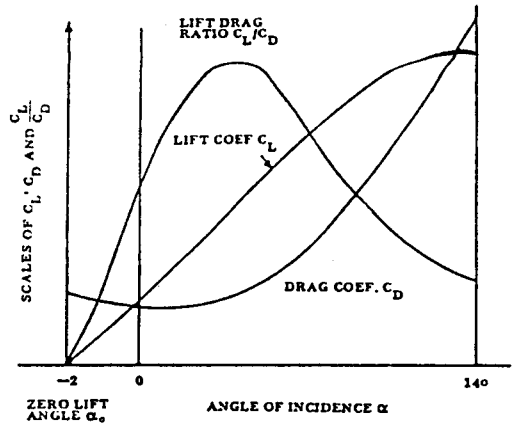


Figure 2.3 Characteristics of Lift and Drag Forces (Source : Reference [14])

If we consider the hull form as a hydrodynamic foil inclined at an angle of attack α to the incoming fluid, we may consider hydrodynamic lift and drag forces to be acting on it in directions perpendicular and parallel to the direction of undisturbed water flow, as indicated in figure 2.4. The velocity of the undisturbed fluid acting on the hull in figure 2.4. is the vector sum of the surge and sway velocities.

$$\bar{u}^2 = u^2 + v^2 \quad (2.2)$$

By definition, the drift angle α is related to the surge and sway velocities by the expression ;

$$\alpha = \tan^{-1} \frac{v}{u} \quad (2.3)$$

As it is not possible to determine, from the standard works on the forces acting on control surfaces, what the precise nature of the lift and drag forces will be on a hull of a particular shape, the model is written under the assumption that the lift and drag forces acting on the ship's hull

where, T_0 is the value of the equilibrium thrust, developed during equilibrium straight ahead motion, the amount of which is just sufficient to balance the hull and rudder drag forces.

When a linear thrust/throttle characteristic is assumed, the thrust equation becomes ;

$$T = K_5 T_b (1 + K_6 S_e) \quad (2.18)$$

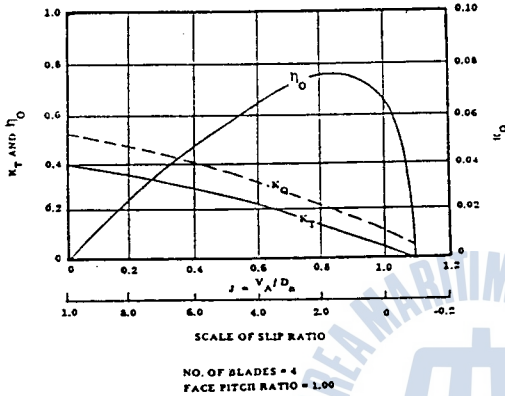


Figure 2.5 Typical Curves of Thrust, Torque and Efficiency for Propeller in Open Water
(Source : Reference [14])

2.2.1.5. Equations of the Ship's Movements

To describe the three degrees of freedom of a ship moving in the flat plane an equilibrium of the two forces and the moment acting on the ship's body will be sufficient.

A starting point is the description of Newton's laws of motions in two orthogonal translations and one rotation direction. In terms of three axes fixed in the earth, the Newtonian equations of the ship are expressed as follows [14][15] ;

$$\begin{aligned} X_0 &= m\ddot{x}_0 \\ Y_0 &= m\ddot{y}_0 \\ N &= I_2\ddot{\psi}_0 \end{aligned} \quad (2.19)$$

where \ddot{x}_0 and \ddot{y}_0 denote the second derivatives of those values with respect to time t , which indi-

cates accelerations of the ship in those direction. In the equations(2.19),

X_0 and Y_0 are total forces in the x_0 and y_0 directions respectively

x_0 and y_0 are the coordinates of the centre of gravity of the ship

m is the mass of the ship

N is total moment about an axis through centre of gravity of ship and parallel to z_0 axis.

I_2 is the moment of inertia of the ship about z_0 axis

ψ is yaw angle which is the angle between the centreline of the ship and the x_0 axis

In spite of the apparent simplicity of equation (2.19), it is simpler to describe the movements of the ship in a system of axes fixed to the ship. The moving axes the origin of which is the centre of gravity of the ship, like the fixed axes x_0 and y_0 , form a right-hand orthogonal system, but with the difference that the origin, O , stays at the centre of gravity of the ship all the time.

As shown in figure 2.6, the orientation of moving axes with respect to the x_0 , y_0 axes is angle of yaw ψ . In the particular case shown in figure 2.6, the angle of yaw ψ is positive. If we convert equations(2.19) from axes fixed in the earth to axes fixed in the moving ship, the forces X and Y in the x and y directions, respectively are expressed in terms of X_0 and Y_0 as follows

$$\begin{aligned} X &= X_0 \cos\psi + Y_0 \sin\psi \\ Y &= Y_0 \cos\psi - X_0 \sin\psi \end{aligned} \quad (2.20)$$

The velocities are ;

$$\begin{aligned} \dot{x}_0 &= u \cos\psi - v \sin\psi \\ \dot{y}_0 &= u \sin\psi + v \cos\psi \end{aligned} \quad (2.21)$$

where u and v denote the components of slip speed along x and y direction respectively.

Differentiation of (2.21) with respect to the time gives ;

$$\begin{aligned} \dot{x}_0 &= \dot{u}\cos\psi - \dot{v}\sin\psi - (u\sin\psi + v\cos\psi) \\ \dot{y}_0 &= \dot{u}\sin\psi + \dot{v}\cos\psi + (u\cos\psi - v\sin\psi) \end{aligned} \quad (2.22)$$

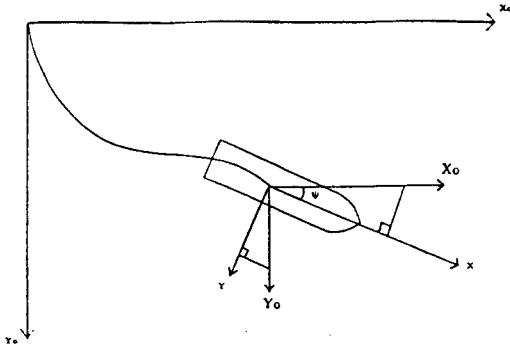


Figure 2.6. Relations Between Axes Fixed in the Earth and Axes Fixed in the Moving Ship
(Source : Reference [14])

If we substitute equation (2.22) in equation (2.19) and insert the resulting values of X_0 and Y_0 in equation (2.20) we obtain ;

$$\begin{aligned} X &= m(\dot{u} - v\dot{\psi}) \\ Y &= m(\dot{v} + u\dot{\psi}) \end{aligned} \quad (2.23)$$

These two equations and the third member of equation (2.19) comprise the equations of motion in the horizontal plane with zero roll, pitch, and heave. The equations of motion are, therefore, expressed as follows ;

$$\begin{aligned} X &= m(\dot{u} - v\dot{\psi}) && \text{surge equation} \\ Y &= m(\dot{v} + u\dot{\psi}) && \text{sway equation} \\ N &= I_z\ddot{\psi} && \text{yaw equation} \end{aligned} \quad (2.14)$$

Each member in the above equations (2.24) represents surge, sway, and yaw movements of the ship respectively.

The equations of motion established in equations (2.24) for a ship with a three degrees of

freedom using axis fixed in the ship may be expressed as follows, the added mass effect being included [13][16] ;

$$\begin{aligned} X &= m_1\dot{u} - m_2v\dot{\psi} \\ Y &= m_2\dot{v} + m_1u\dot{\psi} \\ N &= I_z\ddot{\psi} \end{aligned} \quad (2.25)$$

The added masses in the x and y directions and the added inertia for rotation about the z axis are assumed to remain constant in magnitude.

The forces in x and y directions and moment about z axis are the sum of the external forces acting on the ship, which are made up of propeller, rudder and hydrodynamic forces. Figure 2.3 shows the forces and moments acting on the manoeuvring ship. If we resolve the forces acting on the ship into those parallel to the ship's centreline, the surge equation (2.26) is obtained as follows ;

$$\begin{aligned} m_1\dot{u} - m_2v\dot{\psi} &= T + L_H\sin\alpha - D_H\cos\alpha - L_R\sin\alpha_e \\ &\quad - D_R\cos\alpha_e \end{aligned}$$

therefore,

$$\dot{u} = \frac{1}{m_1} (T + L_H\sin\alpha - D_H\cos\alpha - L_R\sin\alpha_e - D_R\cos\alpha_e + m_2v\dot{\psi}) \quad (2.26)$$

The sway equation is obtained similarly by resolving the forces into those perpendicular to the ship's centreline as follows ;

$$\begin{aligned} m_2\dot{v} + m_1u\dot{\psi} &= -L_H\cos\alpha - D_H\sin\alpha + L_R\cos\alpha_e \\ &\quad - D_R\sin\alpha_e \end{aligned}$$

therefore,

$$\dot{v} = \frac{1}{m_2} (-L_H\cos\alpha - D_H\sin\alpha + L_R\cos\alpha_e - D_R\sin\alpha_e - m_1u\dot{\psi}) \quad (2.27)$$

It is assumed in the above equations that the ship is quasistatic at all times during manoeuvres. The conditions necessary for this assumption to be valid is hardly achieved during normal ma-

B_i denotes bow thruster control

The control B_i is the adjustable variable which is under the control of the operator while the simulation is being carried out.

2.2.2.2 Representation of Steady States of Hydrodynamic Variables

The method of calculating the key variables of surge velocity (u), sway velocity (v) and yaw rate (r) is to establish a steady state value for each, depending on the state of the inputs, and to create a first order differential equation for each variable to obtain the new values. The steady state values are obtained as follows.

(1) Steady State Surge Velocity (U_{ss})

The steady state surge velocity of the ship (U_{ss}) is proportional to the actual shaft speed of the ship's engine. Additionally, the ship slows while she is making a turn, the proportionate loss of speed depending on the square of the yaw rate. When the ship is going astern, its speed is slower for a given shaft speed, because the hull drag is greater in case she is going astern, but the loss of speed in turn may be assumed to be the same proportion.

therefore, we may write :

$$U_{ss} = k(4)N_s - k(5)ur^2 \quad \text{when } u \geq 0 \quad (2.38)$$

$$U_{ss} = k(8)k(4)N_s - k(5)ur^2 \quad \text{when } u < 0 \quad (2.39)$$

(2) Steady State Sway Velocity (V_{ss})

When there is no environment and thruster effects, sway is only induced by the turning effect of the ship. At zero speed, with the ship turning, there is no sway. It may therefore be written :

$$V_{ss} = k(7) \cdot r \cdot w(u) \quad (2.40)$$

where, $w(u)$ is weighting term to be explained in the following section.

(3) Steady State Yaw Rate (R_{ss})

The steady state yaw rate (R_{ss}) is directly affected by the rudder angle. For most ships, the relationship is known to be heavily non-linear [18]. For the present equation, an exponential relationship is used to give the appropriate degree of non-linearity for each ship. Thus,

$$R_{ss} = k(2)\delta^{k(27)} + \beta \quad (2.41)$$

The exponent, $k(27)$, is expected to vary between 0.3 to 0.7 for most merchant ships [18]. The relevant normalised steady state steering characteristics are shown in figure 2.9.

The steady state yaw rate (R_{ss}) is also influenced by the ship's speed. At zero speed the rudder is ineffective. A weighting term $w(u)$ which gives the rudder a reasonable effectiveness at low speeds, increasing at higher speeds, is therefore used, such that [18] :

$$w(u) = \frac{|u|}{k(9)} \quad (2.42)$$

The turning effect of the screws also affects the steady state yaw rate. For right handed single screw ships, the propeller sideforce tends to turn the ship to port when the screw is turning right hand. This turning effect may be expressed as

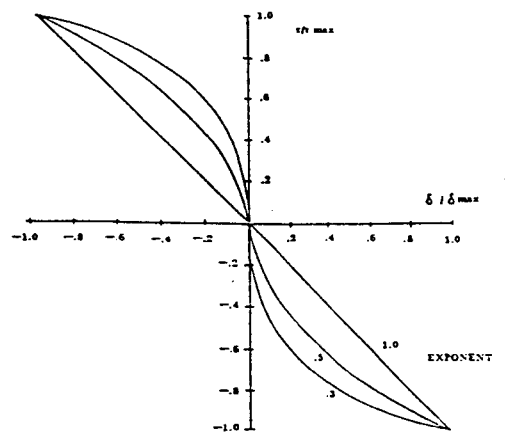


Figure 2.9 Steady State Steering Characteristics (Source : Reference [18])



$$\beta = k(3) (u - k(4)N_s) \quad (2.43)$$

The steady state yaw rate is therefore :

$$R_{ss} = k(2)\delta^{k(27)}w(u) + k(3) (u - k(4)N_s) \quad (2.44)$$

2.2.2.3. Hydrodynamic Equations

The basic form of the equations stated in the previous section is now followed, whereby the time constants associated with each velocity is evaluated, and the first order equations developed for each degree of freedom.

(1) Surge Equation

The time constant for surge velocity is $k(6)$. This time constant needs to be modified for different conditions in a number of ways. When the ship is being decelerated, most ships have a longer time constant. In these equations, a multiplier $k(10)$ is introduced for astern movement. When a ship is making a turn, a greater profile is presented to the water with increasing drift angle. The ship will therefore slow faster. A term Γ_c is introduced to reduce the time constant in T_c as a function of the drift angle.

It may therefore be written :

$$T_c = (1 - k(11) | \alpha |) \quad (2.45)$$

subject to the limit that $T_c > 0.4$

$$d_1 = (U_{ss} - Y(1)) / (k(6)T_c) \quad (2.46)$$

when $Y(1) \leq U_{ss}$

$$d_1 = (U_{ss} - Y(1)) / (k(10)k(6)T_c) \quad (2.47)$$

when $Y(1) > U_{ss}$

where, d_1 denotes surge acceleration

$Y(1)$ denotes surge velocity which equals u

(2) Sway Equation

A simple first order equation is written, relating the steady state value to the actual value :

$$d_2 = (V_{ss} - Y(2)) / k(19) \quad (2.48)$$

where, d_2 denotes sway acceleration

$Y(2)$ denotes sway velocity which equals v

(3) Yaw Equation

The response of the ship to the rudder varies according to the ship's direction of motion and the shaft's direction of rotation. This is reflected in the multiplier for R_{ss} in the first order equations given below :

$$d_3 = (R_{ss} - Y(3)) / k(1) \quad (2.49)$$

when $Y(1) \geq 0, N_s \geq 0$

$$d_3 = (-R_{ss}/2 - Y(3)) / k(1) \quad (2.50)$$

when $Y(1) < 0, N_s < 0$

$$d_3 = (R_{ss}/2 - Y(3)) / k(1) \quad \text{otherwise} \quad (2.51)$$

2.3 Accuracy and Validity of the Mathematical Models

The movement of the ship is predicted by solving the equations for surge, sway and yaw, which were developed in the previous section. The velocities of surge and sway, and the yaw rate are calculated from their respective acceleration equations, by the Euler method.

The model, equations for those three ship's movements, imbedded in the main computer, accepts commands from the instruments on the simulator's bridge, and produces outputs representing the dynamic behaviour of the vessel in response to those commands and to the various environmental influences present within the database. A heavier stress is placed on the mathematical model in port design work than in most other simulation activities, as the mathematical model should be able to represent the behaviour of the ship in all operational conditions to answer the critical questions asked by port designers.

When we consider mathematical model requirements for port design work, a port approach

As for the aids to navigation, there is no plan to place additional navigational aids except for three obstruction lights ; one at the eastern end of the western breakwater and two at both ends of the eastern breakwater.

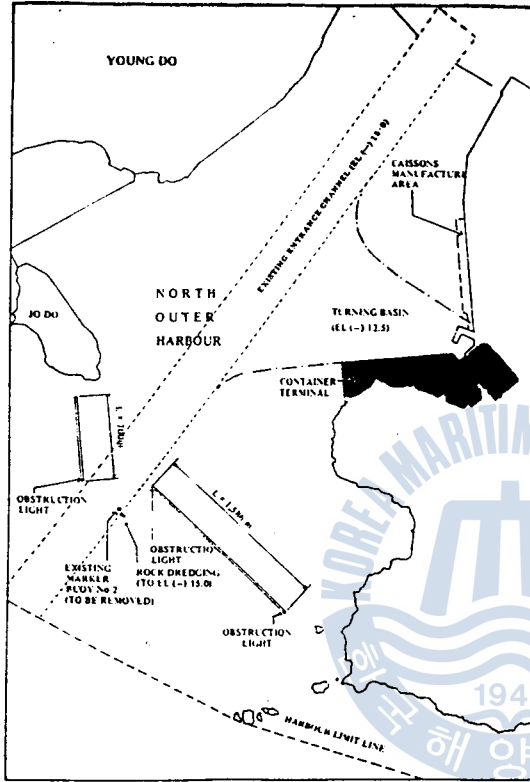


Figure 3.1 Third Stage Development Plan of Busan Harbour
(Source : Reference [30])

As the port has a relatively wide water area, there have not been serious problems in the manoeuvring of large container ships. It is anticipated, however, that after the development of the new container terminal, the container ships using the terminal will face some difficulties in their manoeuvres. Outlined below are the design and operational aspects which need to be examined and assessed, with regard to the safety of the ship, in the newly designed port.

(1) It needs to be examined whether the turning basin near the pier, planned by the Korea Maritime and Port Administration(KMPA), wide enough for the container ships expected use the new terminal, to unberth safely in the worst environmental conditions.

(2) As the construction of two new breakwaters are proposed, it is expected that strong currents exist outside the breakwaters flowing parallel while there are no such currents inside the breakwaters. When a channel end is affected by cross currents, and a vessel enters into a calm water area, the width of the channel needs to be wide enough to take into account the conditions which the vessel is subjected, that is, the bow being no longer subjected to the action of the current, while the stern is still affected. The width between two breakwaters, therefore, must be examined whether it is wide enough for the vessel to transit.

(3) The safety of berthing manoeuvres in the worst environmental conditions needs to be examined.

(4) Chimneys behind the new terminal and the big oil storage tanks around could be used by the pilot of a ship approaching and leaving the terminal. There is no plan to place additional aids to navigation in the existing project. It should, therefore, be examined whether or not it would be safe for the container ships to manoeuvre with the small manoeuvring area with those existing navigational marks, or whether new additional aids to navigation are required.

(5) The safety of departure manoeuvres, from the pier to the pilot station through the new breakwaters, needs to be examined.

3.2 Modelling for Simulation

When we make a hydrodynamic force mathematical model of a ship's manoeuvring behavior we need to measure the force produced by the

propeller and the hydrodynamic forces and moments acting on the ship due to sideslip and turning. Additionally, combinations of these forces and moments must also be measured, as the summation of all the various forces and moments acting on the ship enable a complete mathematical model to be formed [24][25].

However, neither the physical model of the container ship to call at Busan, by which it will be possible to get measurements required, nor the measurements data of a similar ship was available. It has, therefore, been decided to use the heuristic type mathematical model developed by McCallum [18], the validity of which has already been proved in many studies [26][27][28].

The largest ships regularly calling at Busan Container Terminal at present are about 55,000 gross registered tons and 290 metres LOA with a capacity of up to 3,000 TEUs [29]. These ships are approximately Panamax in size. Ship owners building larger ships than these ships will have to give away an important element of flexibility in terms of the routes where such a ship could be employed, instead of gaining some economies of scale. The maximum sized container ships which will call regularly at Busan port in the future are, therefore, unlikely to be larger than the largest ships calling now. Accordingly, a container ship of Panamax size with 297 metres LOA and 30,000 gross tonnage was chosen as the model ship to be simulated. The ship's particulars are shown in table 3.1.

Max. Speed astern	15kts
Maximum Rudder Angle	35
Bow Thruster	1,000HP
Acceleration t(2/3)	190sec
Advance	1040m
Steady State Speed	11.8kts
LOA	297m
Beam	32.2m
No. of Shaft	1
Max. Shaft RPM	95
Max. RPM astern	60
No. of Rudder	1
Rudder Response Time	26sec
Inertia t(1/3)	380sec
Turning Circle	1100m
Transfer	570m

Note : GT ; Gross Tonnage
 LOA ; Length Overall
 Lpp ; Length between Perpendicular
 Max. ; Maximum

(Source : Reference [31])

Table 3.1 Particulars of the Modelled Ship for Simulation

GT	60,000ton
Lpp	274m
Draft	11m
Rotation Direction	righthand
Max. Speed	26kts

3.2.1. Modelling Environmental Parameters

Mathematical models which simulate the forces imparted to a ship by environmental parameters such as currents, winds and waves are essential to ensure the fidelity of the simulation. Among these environmental parameters, wave effect is not included in the environmental model, as Busan harbour is surrounded by land and two breakwaters in which the influence of the wave is assumed negligible.

The method of modelling the wind and current inputs is similar to that employed for the hydrodynamic forces. A steady state value is obtained for the velocity, which would be attained by the ship, and that value is added to the hydrodynamic steady state value, being suitably scaled. As the structure of the equations is essentially unaltered by the additions of further steady state terms, the



therefore, were chosen for the simulation, being regarded as the strongest wind under which the ship should operate. In addition, 30 knots of wind speeds were added to the simulation to take into account the worst case of manoeuvring conditions. In addition to the dominant wind directions of NW and SW, as the ship under the berthing and unberthing operation gets the maximum sideforces by the wind blowing perpendicularly to the pier, two more wind directions of 88 degrees and 268 degrees were chosen for the simulation.

The velocity induced by the wind is assumed to be proportional to the square of the wind strength [18]. The wind vector is resolved into ship axes, and the resulting speeds on O_x and O_y evaluated. The turning effect of the wind depends upon the size and location of the ship's superstructure. Ships with after accommodation will tend to turn to windward, while those with mid-ship accommodation, or with high deck cargo, will tend not to turn, but to drift downwind [33]. Figure 3.6 shows the variables associated with the wind calculations. The relevant equations are (refer to figure 3.6) :

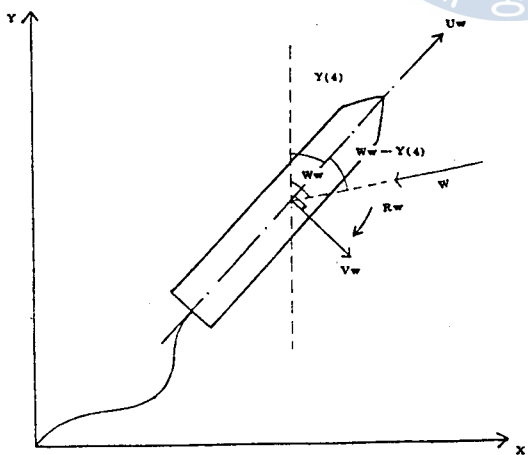


Figure 3.6. Wind Transformation Nomenclature (Source : Reference [18])

$$\begin{aligned}
 U_w &= -k(20) W \cos(W_w/R_{tod} - Y(4)) \\
 V_w &= -k(21) W \sin(W_w/R_{tod} - Y(4)) \\
 R_w &= k(22) W \cos(W_w/R_{tod} - Y(4))
 \end{aligned}
 \tag{3.2}$$

The resulting terms, U_w , V_w , R_w , are then used in the main system equations.

(3) Depth

The necessary size of the gaming area has to be decided before simulation, and the depth database of the water area must be prepared beforehand. As the water area being developed is to be dredged, the depth database is constructed according to the planned depth. The gaming area and the depths of the adjacent area after dredging is shown in figure 3.7.

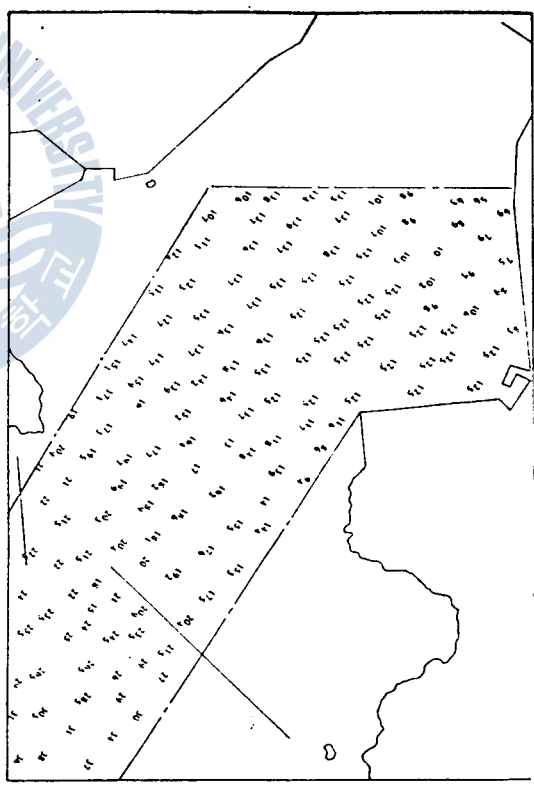


Figure 3.7. Depth of the Gaming Area after Dredging (Sources : Reference [30], [35])



The main shallow water effects experienced by ships are that the approach of the ship's bottom to the sea bed increases the drag, or resistance to motion of the hull. In straight line movement, this will result in [18] ; 1) the ship steady state speed being slower for given engine rpm., 2) the ship accelerating slower, as the engine has to overcome a higher resistance, 3) the ship decelerating faster, as the increased resistance is no longer being overcome by the engine.

The shallow water effects of a ship in turn are rather more complex, but may be summarised as ; 1) the turning circle diameter will in general be increased, 2) the propeller sideforce is increased, as the bottom blades of the propeller are closer to the bottom, 3) the drift angle in turn is usually reduced, although the enhanced sideforce may in some circumstances offset this effect, 4) the loss of speed in turn is reduced [18].

The basic method of approach for the shallow water algorithm is to evaluate the depth under the keel first, and then to draw the appropriate model coefficients which vary as a function of this underkeel clearance.

The underkeel clearance is calculated from ;

$$D_{wm} = (D_w - k(15)) / k(15) \dots\dots\dots (3.3)$$

where, k(15) denotes draught of the model ship

The model coefficients which should be altered are determined by reference to the features which will need to be seen as a result of a decrease in the water depth. In straight line movement, the effects are ; 1) the ship steady state speed is slowed, therefore, k(4) should be reduced, 2) the ship accelerates slower, therefore, k(6) could be increased, 3) the ship decelerates faster, therefore, k(6) should be decreased. In turning, the effects are ; 1) the turning circle diameter becomes larger, therefore, the yaw rate for given rudder angle is reduced, and so k(2) is

reduced. 2) the drift angle is reduced, therefore k(7) should be reduced. 3) there is smaller loss of speed in turn, therefore k(5) is reduced.

The shallow water effects are very small when the depth of water exceeds twice the mean draught of the ship, and get larger as the depth of water approaches the ship's draught. The effects are at their maximum when the ship is about to run aground.

Appropriate expressions for these effects are suggested by McCallum [18] ;

For increasing k ;

$$K_r = 1 + aa(D_{wm})^{-1.2} \dots\dots\dots (3.4)$$

For decreasing k ;

$$k_r' = \frac{1}{1 + aa(D_{wm})^{-1.2}} \dots\dots\dots (3.5)$$

K_r is a multiplying ratio for each individual k value. The value of aa for each individual parameter is taken from the ship's trial data, or from empirical considerations. New coefficients for those affected by shallow water are introduced by omitting the brackets denoting the coefficient number. k2, therefore, represents the shallow water coefficient equivalent of k(2). Where D_{wm} is under 0.1, it is assumed to be equal to 0.1.

Therefore, the coefficients under the shallow water effects are written as follows [18] ;

$$\begin{aligned} k2 &= k(2) / (1 + 0.083D_{wm}^{-1.2}) \\ k4 &= k(4) / (1 + 0.025D_{wm}^{-1.2}) \\ k5 &= k(5) / (1 + 0.060D_{wm}^{-1.2}) \\ k6A &= k(6) \times (1 + 0.036D_{wm}^{-1.2}) \\ k6D &= k(6) / (1 + 0.048D_{wm}^{-1.2}) \\ k7 &= k(7) / (1 + 0.170D_{wm}^{-1.2}) \end{aligned} \dots\dots\dots (3.6)$$

(4) Tug

In port development it is necessary for economic and safety reasons to ensure tug escort and assistance for large vessels in transit through the harbour [36]. In addition, tugs will be needed for



changes in direction take place. The program then fills in the area between the points to the height specified in metres, making curtains which represent the coastline or piers. The mountains were made in such a way that they consist of curtains with different heights, the heights of which change to give the effect of mountains to the viewer's eyes.

The database for the radar picture, which is treated by the radar scene generating program, uses the same data as the visual scene in X, Y coordinates, but is simpler in form, as the three dimensional and height effects are not required.

3.3.2 Run Schedule

Four types of manoeuvres; unberthing, entering through breakwaters, berthing, and departure, were scheduled to be examined. Unberthing manoeuvres were divided into two types. Unberthing and berthing manoeuvres were examined in flood tide only, as the difference between flood and ebb current will be of negligible magnitude in front of the container pier. Other manoeuvres were examined in both ebb and flood current. Entering manoeuvres through the new breakwaters were divided into two types; one without a sea buoy and the other with a sea buoy.

Eight groups of simulated runs were performed, and each group was followed by 6 familiarisation runs. In total, 116 runs were performed, of which 68 runs were for actual examination and 48 were familiarisation runs. The simulated runs were performed by a former Cardiff pilot employed by Maritime Dynamics Ltd., and a navigator with five years' sea experience. Both the pilot and the mariner were selected from those who had been involved in port design simulation for more than 6 months. Detailed run schedule is shown in table 3.3.

Table 3.3. Run Schedule

Manoeuvre	Run Numbers	Number of Runs	Current	Wind Direction	Wind Speed
unberthing (A type)	B1-B13	9	flood (predicted)	SW, W NW, E	27 kts 30 kts
unberthing (B type)	B30k-B37	10	flood (predicted)	SW, W NW, E	27 kts 30 kts
entering through breakwaters	B41-B49	8	ebb flood (predicted)	SW, NW	30 kts 35 kts
“ (with sea buoy)	B50-B57	8	“	“	“
entering through breakwaters	B58-B66	9	(maximum 2.4 kts)	“	“
berthing	B67-B74	8	flood (predicted)	SW, W NW, E	27 kts 30 kts
departure	B14-B21	8	flood (predicted)	“	“
departure	B22-B29	8	ebb (predicted)	“	“

(Source : Depicted by the Author)

3.4 Analysis of the Simulation Results

The results of each run are explained and analysed group by group. Among 68 simulated runs, the plots of the significant runs are shown in this section and appendix.

3.4.1 Unberthing Simulation in the Turning Basin

19 unberthing runs were performed to examine whether the turning basin planned by KMPA is sufficiently wide for the modelled container ship which is expected to use the new terminal.

The worst cases of unberthing manoeuvres are considered to be those with the vessel starboard side to No. 1 berth. Accordingly, unberthing manoeuvres from No. 1 berth only were examined.

Since the currents near the pier are of negligible magnitude, the manoeuvres were performed in a flood current only, ignoring the difference between ebb and flood. In addition to the dominant wind directions of NW and SW of the Busan, easterly and westerly winds were also tested, as those winds blowing perpendicular to the pier are considered to be the most influential to a berthing ship; wind speeds of 27 knots and 30 knots were given.

In the first place, nine A type unberthing manoeuvres(run B1—run B13), in which the ship turns to port directly, as she gets out from No.1 berth, were examined.

From the nine different unberthing manoeuvres simulated, it was concluded that the proposed dredging area was not wide enough for the modelled container ship to perform unberthing manoeuvres safely, especially when the wind blew from the east on the vessel's beam. It is necessary, therefore, to adjust the dredging area unless another safe unberthing strategy is found.

For this reason, a different type(B type) of unberthing manoeuvre suggested by the pilot was examined, in which the ship goes astern from the berth to the turning area in front of No. 2 berth, where the ship makes 180 degrees starboard turn to get out of the turning basin. 10 runs had been performed in the winds blowing from four different directions.

From the above 19 runs, it was found that the dredging area planned by KMPA was not wide enough, for the modelled container ship to berth in such a way that the ship turns to port as she gets out from No. 1 berth, especially in the easterly wind.

The alternative manoeuvring strategy, in which the ship goes astern from No. 1 berth to the turning area in front of No. 2 berth (where the ship turns 180 degrees to starboard), was found to be safer than the former method for the following

three reasons :

1) The closest point of the ship's path to the 12.5 metres dredging line is far greater than the previous case.

2) As the ship's stern is usually more vulnerable to collisions with the quay structures than the ship's bow, it is more desirable to get her stern out first from the berth for the ship's safety.

3) Fewer tugs are needed than for the previous case.

It is, therefore, recommended that pilots should take the second unberthing strategy, in which the ship goes astern from the berth and turns 180 degrees to starboard, right after the ship's bow is abeam to the middle of No. 2 berth.

3.4.2 Entering Manoeuvres Through the new Breakwaters

A total of 25 runs, which start from the pilot station to be completed before No. 3 buoy, have been carried out to examine the following :

1) the safety of the ship's entering through the new breakwaters under the worst current and wind conditions,

2) the necessity of placing a sea buoy outside the new breakwaters,

3) other navigational problems in connection with the construction of the new breakwaters.

Since southwesterly and northeasterly winds blow almost parallel to the predicted currents near the breakwaters, those winds are expected to affect entering manoeuvres the most. Therefore, entering manoeuvres through the new breakwaters were examined in a southwesterly and northeasterly wind. Different from the berthing and unberthing, which can be delayed when the weather is very rough, ships have to enter the harbour even when it is a gale. 30 knots wind, therefore, was regarded as the strongest wind under which ships should enter the harbour. In addition, a gale wind of 35 knots was added to the simulation to take into account the worst

manoeuvring of a ship through the breakwaters. The result of run B60 is shown in figure 3.12. This result coincides with the work of Maquet [39], in which ship manoeuvres were found to be more precise when pilots knew in advance the directions and speeds of currents. It is, therefore, strongly recommended that the Korean Hydrographic Office carry out a detailed survey of the currents near the new breakwaters once they have been constructed.

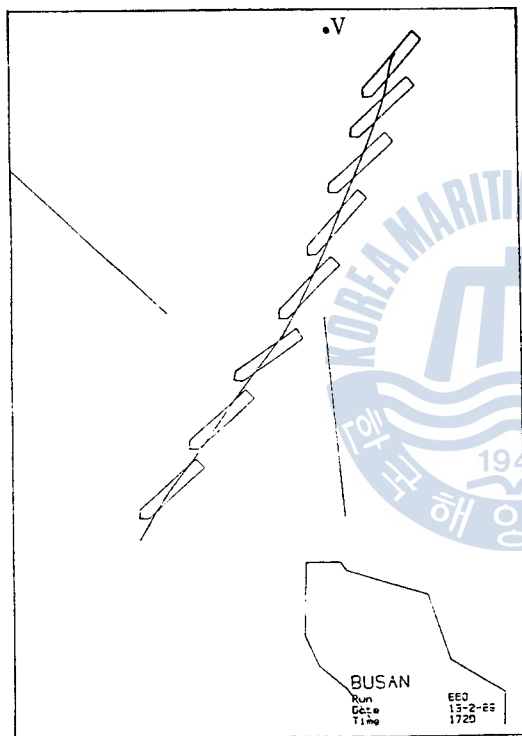


Figure 3.12. The Result of Run B60

3. 4. 3 Berthing Manoeuvres

Eight arrival manoeuvres (run B67—run B74) were performed to examine the safety of the berthing manoeuvres in the worst possible environmental conditions to ascertain whether it is necessary to place additional navigational marks near the pier. The berthing manoeuvres onto No. 1 berth were examined. Each manoeuvre started from

No. 3 buoy at a speed of about 7 knots.

As the currents near the pier are of negligible magnitude, the manoeuvres were only carried out in the flood tide, ignoring any differences between ebb and flood tide. Easterly and westerly winds were introduced into the test runs in addition to the dominant wind directions of the NW and SW of the Busan, as those winds blowing perpendicular to the pier are considered to give the biggest adverse effect to the ship's berthing. The wind speeds of 27 knots and 30 knots were used.

There were no problems experienced in berthing the ship on the terminal. Two tugs were required for berthing except when the wind was blowing from the east, in which case four tugs were required to manoeuvre the ship against the wind blowing abeam of the ship. Chimneys around KOMMATRI were found to be good leading marks for berthing ships. No additional navigational marks were seen to be required.

3. 4. 4 Departure Manoeuvres from the Pier to the Pilot Station

To examine the safety of departure manoeuvres, 16 runs, from No. 1 berth to the pilot station were performed under different environmental conditions. To begin with, eight runs (run B14—run B21) were performed in a flood tide.

In the same manner as the unberthing manoeuvres, in addition to the dominant wind directions of NW and SW of the Busan, easterly and westerly winds were also tested; the wind speeds of 27 knots and 30 knots were used. Unlike the entering manoeuvres through the breakwaters, a wind speed of 30 knots was regarded as the worst case, since ships are not allowed to unberth under the gale conditions normally.

Another eight runs (run B22—run B29) were performed in an ebb tide. As the currents are almost parallel to the channel and the current

near the pier are of negligible magnitude, there were no significant differences between departure manoeuvres in the flood current and those in the ebb current.

It was found that there were no difficulties for the modelled container ship to leave the terminal through the new breakwaters, even in the worst wind and current combinations.

4. CONCLUSIONS

Factors which influence the port and waterway design are divided into four groups which are : ship's inherent factors such as the size and manoeuvrability of the vessel ; environmental factors such as winds, waves and currents; human factors and aids to navigation factors. These factors should be dealt with simultaneously when designing a port or waterway. The human element within the ship control system requires manoeuvring experiments for port and waterway design to be conducted on a real time scale. Accordingly, dynamic ship simulation, in which human ship operators are involved, is regarded as one of the most useful methods within the current state of knowledge. The concept of the microcomputer aided port design simulation together with the analysis of the ship mathematical models was introduced in this paper.

The Third Stage Development Plan of Busan port for a new container terminal was investigated by the simulation after the port design simulation methodology was introduced.

A container ship of Panamax size with 297 metres LOA and 60,000 gross tonnage was chosen as the model ship to be simulated. Eight groups of simulated runs were performed by an experienced former Cardiff pilot and a navigator, both of whom had been involved in port design simulation for at least 6 months.

Among 68 actual runs, nineteen runs were performed to examine whether the turning basin planned by the Korea Maritime and Port Administration is sufficient for the container ships which are expected to use the terminal. A total of 25 runs, from the pilot station to No. 3 buoy, were performed to examine ; the safety of the entering manoeuvres through the new breakwaters under the worst possible current and wind conditions ; the need to place a sea buoy outside the new breakwaters and the other navigational problems related to the construction of the new breakwaters. Eight arrival runs, from No. 3 buoy to No. 1 berth, were performed to examine the safety of berthing manoeuvres in the worst possible environmental conditions and to ascertain whether additional navigational marks are required. Sixteen runs, from No. 1 berth to the pilot station, were performed to examine the safety of departure manoeuvres.

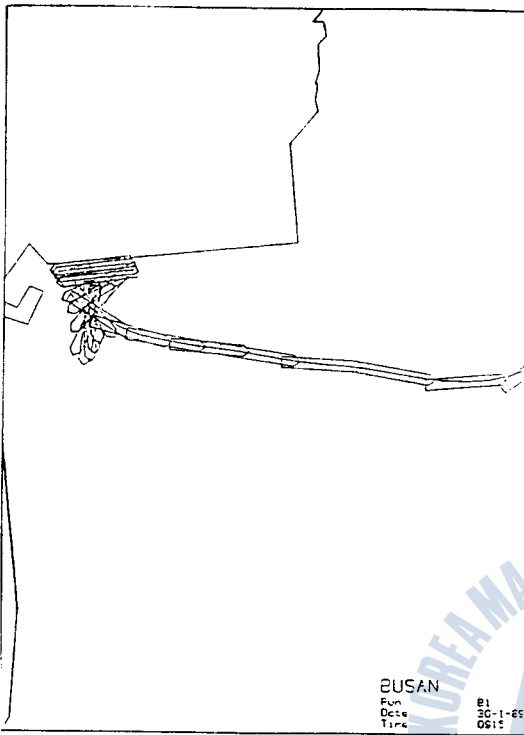
The findings from the simulation study are as follows :

1) It was found that the proposed dredging area was not sufficiently wide enough for the container ship to perform A type unberthing (in which the ship turns to port as she manoeuvres away from No. 1 berth with the assistance of tugs), especially in the strong E'ly wind. The alternative manoeuvring strategy of B type, in which the ship goes astern from No. 1 berth to the turning area in front of No. 2 berth (where the ship turns 180 degrees clockwise), was found to be safer than the A type).

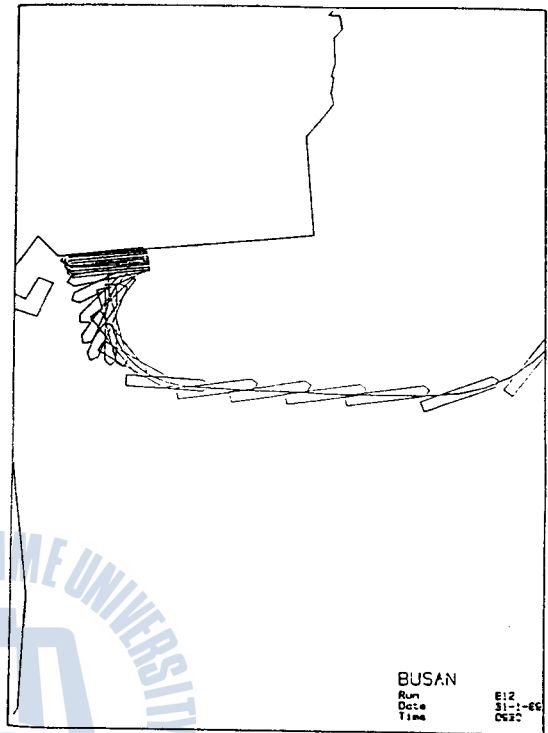
2) There are no serious problems for the modelled container ship to enter through the breakwaters even in the worst expected combination of wind and current. Nevertheless, the lack of accuracy in the estimation of the ship's position during the initial stage of the manoeuvres caused manoeuvring difficulties in that the ship drifted

- Korea Port Phase Three Development Study – Final Report*, Volume 1, Lyon Associates Ltd., Seoul, 1981.
- 24) McCallum, I. R., *A New Approach to Manoeuvring Ship Simulation*, Doctoral thesis of City University, London, 1976.
- 25) Kettenis, D. L., “On the Mathematical Description of Ship Manoeuvring”, Netherland Ship Model Basin, Wegeningen, Holland.
- 26) Maritime Dynamics, *Port of Sunderland Simulation Study Report*, Publication of Maritime Dynamics Ltd., Llantrisant, U. K., July 1987.
- 27) Maritime Dynamics, *Second Severn Crossing Ship Simulator Study Report*, Publication of Maritime Dynamics Ltd., Llantrisant, U. K., March 1989.
- 28) Maritime Dynamics, *Avimar Systems – Mathematical Manoeuvring Models Progress Report No. 4*, Publication of Maritime Dynamics Ltd., Llantrisant, U. K., Oct. 1984.
- 29) Woodward – Clyde Consultants, *Study on Maximised Utilisation of Existing Container Terminal and Operational System*, Busan Container Terminal Operation Company, 1987, pp. 29~39.
- 30) Lyon Associates Inc. and Korea Engineering Consultants Corporation, *General Plan of Busan Outer Harbour Civil Project No. 4*, Korea Maritime and Port Administration, Seoul, 1984.
- 31) Maritime Dynamics, *Notebook on Mathematical Models*, Maritime Dynamics Ltd., Llantrisant, U.K., 1987.
- 32) Hydrographic Offices of Republic of Korea, *Tidal Current Charts (Busan to Yeosu) Pub. No 1420*, Department of Transport, Seoul, 1982.
- 33) McIlroy, W., “Ship Manoeuvring Response – Simulation Studies at CAORF”, *Proceedings of Fifth CAORF Symposium*, CAORF, New York May 1983.
- 34) Central Meteorological Office of Republic of Korea, *Climatic Table of Korea*, Vol. 1, Seoul 1982.
- 35) Hydrographic Office of Republic of Korea *Harbour Chart (Approaches to Pusan Hang Pub. No. 228*, Department of Transport, Seoul 1972.
- 36) Puglisi, J., “Use of Simulation Techniques Capabilities And Methodology Required for Harbour/Waterway Design Studies”, Paper Presented to *The Second International Conference Computer Aided Design, Manufacture and Operation in the Marine and Offshore Industries*, Kings Point, New York, 1988.
- 37) Atkins, D. A., Bertsche, W. R., “Evaluation of the Safety of Ship Navigation in Harbours” *Proceedings of Spring Meeting/STAR Symposium*, Coronado, California, 1980, p. 74.
- 38) Smith, M. W., Multer, J., Schroeder, K., “Simulator Evaluation of Turn Lighting Effectiveness for Nighttime Piloting”, *Proceedings of the Fifth CAORF Symposium*, CAORF, New York, May 1983.
- 39) Maquet, J. F., “Application of Investigation Methods to the Layout of Port Structures and Water Surfaces”, *Proceedings of the Symposium on the Aspects of Navigability of Constrained Waterways, Including Harbour Entrances* Vol. 3, paper No. 20, delft, Netherlands, 1978.

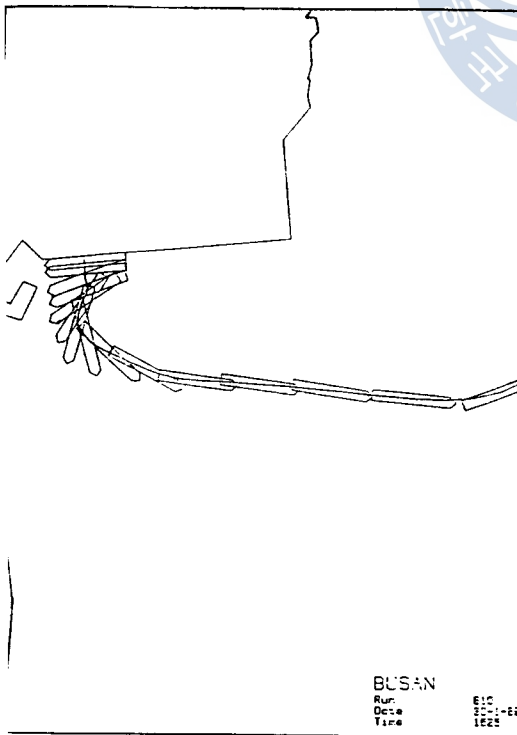
APPENDIX



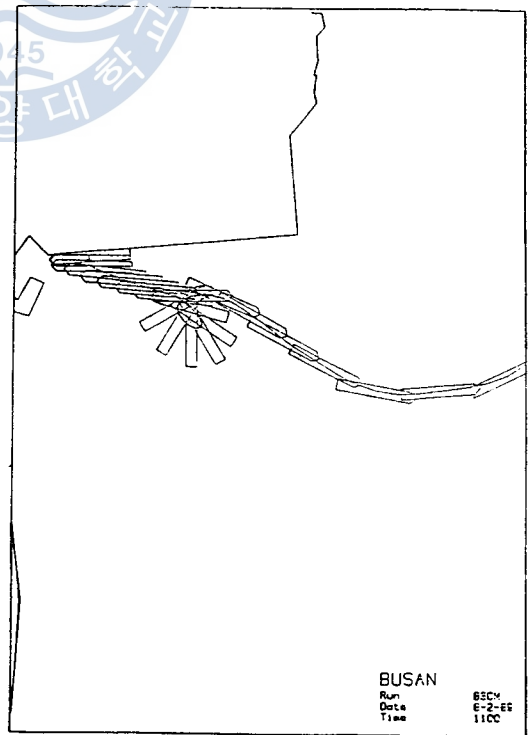
The Result of Run B1



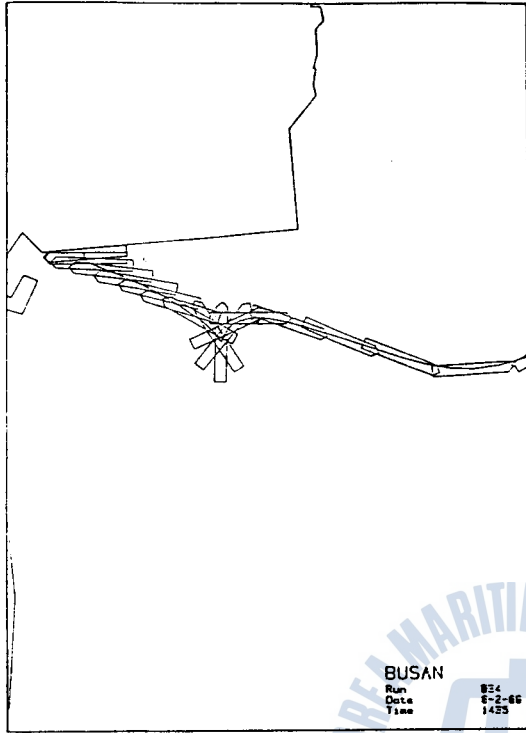
The Result of Run B12



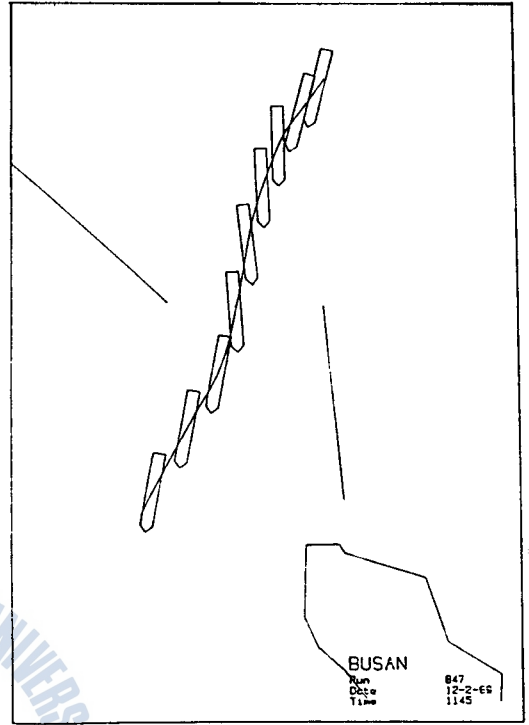
The Result of Run B10



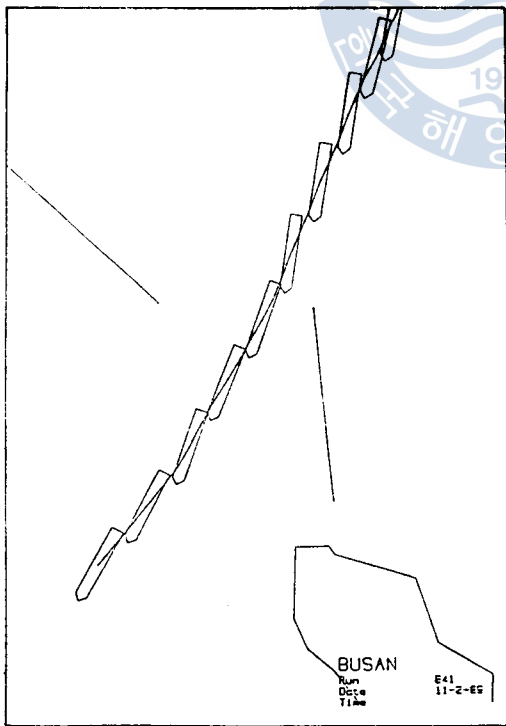
The Result of Run B30M



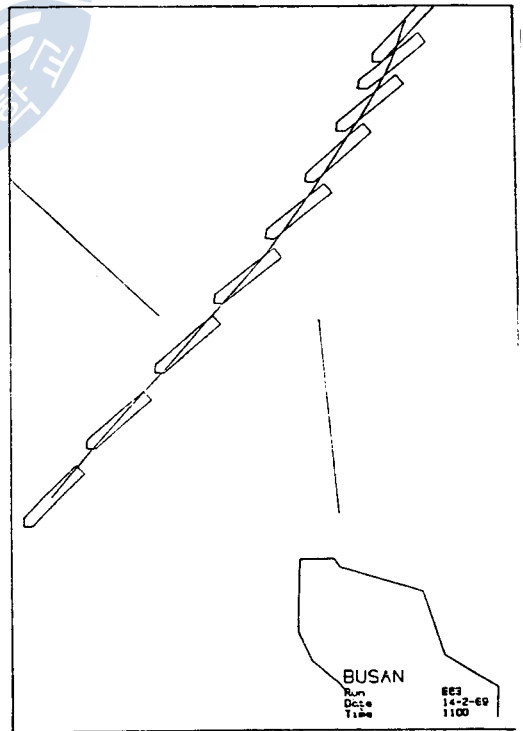
The Result of Run B34



The Result of Run B47



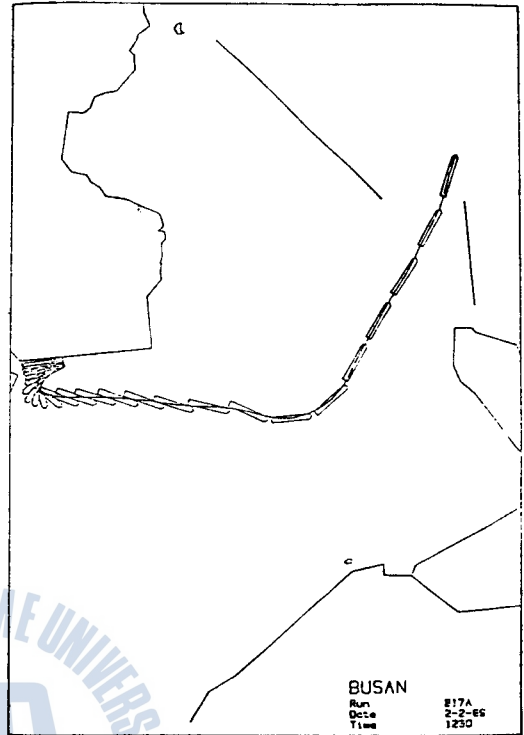
The Result of Run B41



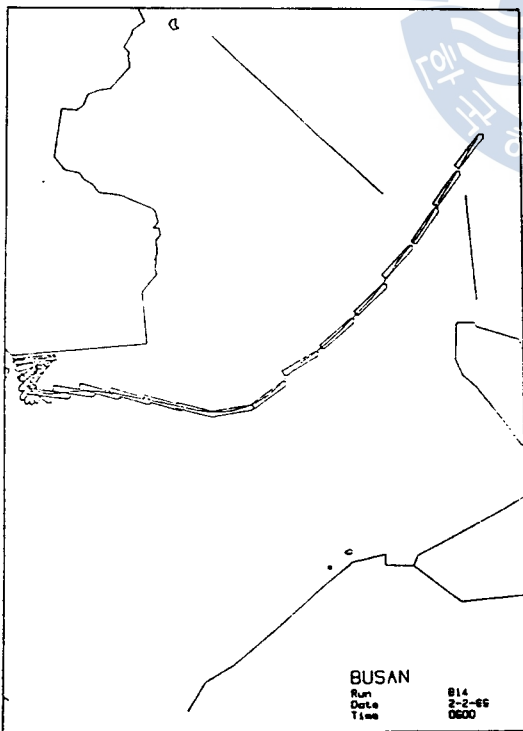
The Result of Run B63



The Result of Run B67



The Result of Run B17A



The Result of Run B14

